A&A manuscript no.
(will be inserted by hand later)

Your thesaurus codes are:
05 (08.05.1; 08.06.3; 08.08.2; 10.07.3 NGC 6388; 10.07.3 NGC 6441)

ASTRONOMY AND ASTROPHYSICS

February 1, 2008

Blue horizontal branch stars in metal-rich globular clusters. I. NGC 6388 and NGC 6441⋆

S. Moehler[1], A. V. Sweigart[2], and M. Catelan[2,⋆⋆,⋆⋆⋆]

[1] Dr. Remeis-Sternwarte, Astronomisches Institut der Universität Erlangen-Nürnberg, Sternwartstr. 7, 96049 Bamberg, Germany
e-mail: ai13@sternwarte.uni-erlangen.de

[2] NASA Goddard Space Flight Center, Code 681, Greenbelt, MD 20771, USA
e-mail: sweigart@bach.gsfc.nasa.gov, catelan@virginia.edu

submitted April 9, 1999; revised version July 29, 1999

Abstract. We report the first results of an ongoing spectroscopic survey of blue horizontal branch stars in the metal-rich ([Fe/H] $\simeq -0.5$) globular clusters NGC 6388 and NGC 6441. Based on data obtained with the ESO–*New Technology Telescope* (NTT), we provide gravities and temperatures for four stars in NGC 6388 and three stars in NGC 6441. These results are marginally inconsistent with the predictions of canonical evolutionary theory, but disagree strongly with all non-canonical scenarios that explain the sloped horizontal branches seen in the colour-magnitude diagrams of these clusters.

Key words: Stars: early-type – Stars: fundamental parameters – Stars: horizontal-branch – globular clusters: individual: NGC 6388 – globular clusters: individual: NGC 6441

1. Introduction

The metal-rich globular clusters play a fundamental rôle in determining the formation history of our Galaxy (e.g. Minniti 1995, 1996; Ortolani et al. 1995; Zinn 1996; Barbuy et al. 1998; Rich 1998). Moreover, they provide a crucial template for interpreting the integrated spectra of elliptical galaxies and for understanding the evolution of old metal-rich stellar systems. The horizontal branch (HB) stars in the metal-rich clusters are particularly important, since they provide a standard candle for determining distances (and hence ages) and are believed to be the major contributors to the UV-upturn phenomenon (e.g. Caloi 1989; Greggio & Renzini 1990, 1999; Bressan et al. 1994; Dorman et al. 1995; Yi et al. 1998).

Recent *Hubble Space Telescope* (HST) observations have found that the metal-rich globular clusters NGC 6388 (C1732–447) and NGC 6441 (C1746–370) ([Fe/H] = −0.60 and −0.53, respectively; Harris 1996) contain an unexpected population of hot HB stars and therefore exhibit the well-known second parameter effect (Rich et al. 1997). Most surprisingly, the mean HB luminosity at the top of the blue HB tail is roughly 0.5 mag brighter in V than the red HB "clump," which itself is strongly sloped as well. Differential reddening cannot be the cause of these sloped HB's (Piotto et al. 1997; Sweigart & Catelan 1998; Layden et al. 1999).

The second parameter effect has often been attributed to differences in age or mass loss on the red giant branch (RGB). However, canonical HB simulations show that increasing the assumed age or RGB mass loss moves an HB star blueward in the V, $B-V$ plane but does not increase its luminosity. Thus some other second parameter(s) must be causing the sloped HB's in NGC 6388 and NGC 6441 (Sweigart & Catelan 1998, hereafter SC98).

Three non-canonical scenarios have been suggested to explain the sloped HB's and long blue HB tails in these metal-rich globular clusters (SC98):

1. **High cluster helium abundance scenario**: Red HB stars evolve along blue loops during most of their HB lifetime. For larger than "standard" helium abundances Y, these loops become considerably longer, reaching higher effective temperatures and deviating more in luminosity from the zero-age HB (ZAHB). If the cluster stars form with sufficiently high Y ($\gtrsim$ 0.4), the HB will slope upward (Catelan & de Freitas Pacheco 1996), as observed in NGC 6388 and NGC 6441. However, this scenario also predicts a much larger value for the number ratio R of HB to RGB stars than the value recently obtained by Layden et al. (1999) for NGC 6441. Thus a high primordial helium abundance seems to be ruled out as the cause of the sloped HB's and will not be considered further in this paper.

Send offprint requests to: S. Moehler

⋆ Based on observations collected at the European Southern Observatory (ESO Nº 61.E-0361)

⋆⋆ Hubble Fellow.

⋆⋆⋆ Visiting Scientist, Universities Space Research Association.

2. **Rotation scenario**: Rotation during the RGB phase can delay the helium flash, thereby increasing both the final helium-core mass and the amount of mass loss near the tip of the RGB. The net effect is to shift a star's HB location towards higher effective temperatures and luminosities, depending on the amount of rotation. This scenario predicts a sloped HB with the shift towards higher luminosities (and hence lower gravities) increasing with effective temperature (Rood & Crocker 1989).
3. **Helium-mixing scenario**: The observed abundance variations in globular cluster RGB stars show that these stars are able to mix nuclearly processed material from the vicinity of the hydrogen-burning shell out to the surface (e.g. Kraft 1994). In particular, the observed Al enhancements indicate that the mixing can penetrate into the H-shell, thus leading to the dredge-up of helium. The resulting increase in the envelope helium abundance produces an HB morphology that slopes upward towards brighter luminosities with increasing effective temperature (Sweigart 1997; SC98). The shift towards lower than canonical gravities due to helium mixing reaches a maximum between 10,000 K and 20,000 K. No shift is predicted for the hottest HB stars (>20,000 K), where the H-shell is inactive and the luminosity is therefore unaffected by helium mixing (Sweigart 1997). This scenario might also help to explain the low gravities of the blue HB stars found in several metal-poor globular clusters (Moehler 1999 and references therein), although Grundahl et al. (1999) have recently provided some caveats about it. They do note, however, that "helium mixing stands out as the best candidate to explain the anomalous HB morphology of the metal-rich globular clusters NGC 6388 and NGC 6441".

These scenarios make different predictions for the surface gravities of HB stars which can be tested observationally. We started a program to obtain spectroscopic observations with this goal in mind and report here on our first results. In Sect. 2 we describe our observations and the employed data reduction techniques; in Sect. 3 the procedure adopted to derive the atmospheric parameters of the programme stars is outlined. Finally, we discuss our results and their consequences in Sect. 4.

2. Observations and Data Reduction

We selected our targets from the HST *Wide Field and Planetary Camera–2* (WFPC2) images of Rich et al. (1997) which were convolved with a "seeing" of 1″ in order to allow the selection of stars suitable for *ground-based* spectroscopic observations. We took spectra of four stars in NGC 6388 and three stars in NGC 6441 (see Table 1). Unfortunately, due to rather mediocre weather conditions we could not observe more stars during our *New Technology Telescope* (NTT) observing run.

We used only the blue channel of the *ESO Multi-Mode Instrument* (EMMI) at the NTT, since the use of the two-channel mode leads to destructive interference around the H_β line. We obtained medium resolution spectra to measure Balmer line profiles and helium line equivalent widths. We used grating #4 (72 Å mm^{-1}) and a slit width of 1.″0, keeping the slit at parallactic angle for all observations. Seeing values varied between 0.″8 and 1.″5. The CCD was a Tek 1024 × 1024 chip with $(24\,\mu\mathrm{m})^2$ pixels, a read-out-noise of 5.7 e$^-$ and a gain of 2.84 e$^-$ADU^{-1} (where as usual "ADU" stands for analog-to-digital-units).

For calibration purposes we observed each night ten bias frames and ten dome flat-fields with a mean exposure level of about 10,000 ADU each. In the beginning of each night we took a long HeAr exposure for wavelength calibration. Due to the long exposure times for the Ar spectrum we only obtained He calibration spectra during the night (before and after each science observation) and determined the offsets relative to the HeAr spectrum (from which the dispersion relation was derived) by correlating the two spectra. For the second night (and part of the third night) we could not obtain *any* wavelength calibration spectra due to technical problems. To correct any spectral distortions we used HeAr spectra from the first night for those data. The FWHM of the HeAr lines was measured to be 5.67±0.2 Å and was used as instrumental resolution. As flux standard stars we used LTT 7987 and EG 274.

We averaged the bias frames of the three nights and used their mean value instead of the whole frames as there was no spatial or temporal variation detectable. To correct the electronic offset we adjusted the mean bias by the difference between the mean overscan value of the science frame and that of the bias frame. The dark currents were determined from several long dark frames and turned out to be negligible ($5.6 \pm 4.2\ \frac{e^-}{hrpx}$).

The flat fields were averaged separately for each night, since we detected a slight variation in the fringe patterns of the flat fields from one night to the next (below 5%). We averaged the flat fields and then determined the spectral energy distribution of the flat field lamp by averaging the flat fields along the spatial axis. This one-dimensional "flat field spectrum" was then heavily smoothed and used afterwards to normalize the dome flats along the dispersion axis.

For the wavelength calibration we fitted 3$^{\mathrm{rd}}$-order polynomials to the dispersion relations of the HeAr spectra. They were adjusted for eventual offsets by cross-correlating them with the He spectra belonging to the science frame. We rebinned the frames two-dimensionally to constant wavelength steps. Before the sky fit the frames were smoothed along the spatial axis to erase cosmics in the background. To determine the sky background we had to find regions without any stellar spectra, which were sometimes not close to the place of the object's spectrum. Nevertheless the flat field correction and wavelength cal-

Table 1. Target list. Positions and photometry are from Piotto (priv. comm.)

Cluster	Star	α_{2000}	δ_{2000}	V [mag]	$B-V$ [mag]
NGC 6388	WF2–42	$17^h36^m21\overset{s}{.}4$	$-44°42'56''$	17.440	+0.334
NGC 6388	WF3–14	$17^h36^m23\overset{s}{.}5$	$-44°43'11''$	16.914	+0.333
NGC 6388	WF3–15	$17^h36^m24\overset{s}{.}1$	$-44°43'15''$	16.896	+0.432
NGC 6388	WF4–20	$17^h36^m20\overset{s}{.}9$	$-44°45'10''$	17.183	+0.341
NGC 6441	WF2–24	$17^h50^m08\overset{s}{.}5$	$-37°04'09''$	17.567	+0.386
NGC 6441	WF3–16	$17^h50^m06\overset{s}{.}2$	$-37°02'50''$	17.683	+0.558
NGC 6441	WF3–17	$17^h50^m04\overset{s}{.}5$	$-37°02'20''$	17.643	+0.499

ibration turned out to be good enough that a linear fit to the spatial distribution of the sky light allowed the sky background at the object's position to be reproduced with sufficient accuracy. This means in our case that after the fitted sky background was subtracted from the unsmoothed frame we do not see any absorption lines caused by the predominantly red stars of the clusters. The sky-subtracted spectra were extracted using Horne's (1986) algorithm as implemented in MIDAS (Munich Image Data Analysis System).

Finally the spectra were corrected for atmospheric extinction using the data of Tüg (1977). The data for the flux standard stars were taken from Hamuy et al. (1992) and the response curves were fitted by splines.

3. Atmospheric Parameters

To derive effective temperatures, surface gravities and helium abundances we fitted the observed Balmer and helium lines with stellar model atmospheres. Beforehand we corrected the observed spectra for wavelength shifts introduced by radial velocities and the lack of appropriate wavelength calibration frames (see Sect. 2), derived from the positions of the Balmer lines. The individual spectra for each star were then co-added and normalized by eye and are plotted in Fig. 1. For the normalization we assumed that the observed noise is mostly caused by photon noise. However, to account for the possibility of faint unresolved metal lines we tried to place the continuum line at the upper region of the scatter.

To establish the best fit we used the routines developed by Bergeron et al. (1992) and Saffer et al. (1994), which employ a χ^2 test. In addition the fit program normalizes model spectra *and* observed spectra using the same points for the continuum definition. The σ necessary for the calculation of χ^2 is estimated from the noise in the continuum regions of the spectra.

We computed model atmospheres using ATLAS9 (Kurucz 1991, priv. comm.) and used Michael Lemke's version[1] of the LINFOR program (developed originally by Holweger, Steffen, and Steenbock at Kiel University) to compute a grid of theoretical spectra which include the

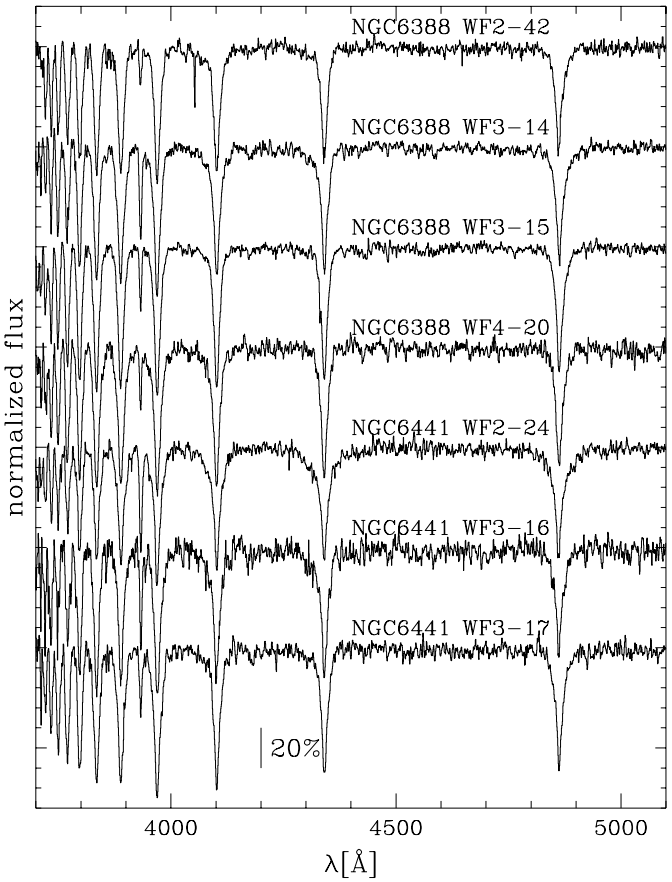

Fig. 1. Normalized spectra for the programme stars

Balmer lines H_α to H_{22} and He I lines. The grid covered the range 7500 K $\leq T_{\rm eff} \leq$ 20,000 K, $2.5 \leq \log g \leq 5.0$, $-3.0 \leq \log \frac{n_{\rm He}}{n_{\rm H}} \leq -1.0$, at metallicities of [M/H] = −0.75 and [M/H] = −0.50. To check the effects of metallicity we fitted the spectra at $\log \frac{n_{\rm He}}{n_{\rm H}} = -1.0$ using model spectra with [M/H] = −0.50 and [M/H] = −0.75. The fit results for the two metallicities were almost identical: $T_{\rm eff}$ and $\log g$, respectively, increased by at most 1% and 0.03 dex from [M/H] = −0.50 to −0.75 (except for NGC 6441 WF3–16, where $\Delta T_{\rm eff}$ and $\Delta \log g$ were 1.6% and 0.07 dex, respectively). All further analysis was therefore performed for a fixed metallicity of [M/H] = −0.50.

[1] http://www.sternwarte.uni-erlangen.de/~ai26/linfit/linfor.html

As none of the programme stars showed any He absorption lines we first fitted all spectra at two fixed helium abundances, $\log \frac{n_{\rm He}}{n_{\rm H}} = -1.0$ and -2.0, using the Balmer lines H_β to H_{10} (except H_ϵ to avoid contamination by the Ca II H line). When defining the fit regions we took care to extend them as far as possible while avoiding any predicted strong He I lines ($\lambda\lambda$ 4026 Å, 4388 Å, 4921 Å) which might be present at the noise level although undetected by eye. Such lines would distort the fit: Fitting regions of strong He I lines while keeping the helium abundance fixed will result in erroneous results for $T_{\rm eff}$ and $\log g$ if the helium abundance of the model atmospheres is not identical with that of the star. The results are listed in Table 2.

As the stars are rather cool it is not obvious from the spectra on which side of the Balmer maximum they lie. However, the strength of the Ca II K line can be used to distinguish between the "hot" and the "cool" solution: the observed equivalent width of this line has stellar and interstellar contributions. As the clusters are highly reddened – $E(B-V) = 0.40$ and 0.44 for NGC 6388 and NGC 6441, respectively (Harris 1996) – *the observed equivalent width has to be significantly larger than the one predicted by the model atmosphere* for [M/H] = −0.5. In Table 2 we list the atmospheric parameters for all stars together with the measured and predicted equivalent widths for the Ca II K line. *The comparison between observed and predicted values places all ambiguous stars on the hot side of the Balmer maximum.*

For those stars that are hotter than 9,500 K we finally fitted the Balmer lines mentioned above together with those regions of the spectra where the He I lines $\lambda\lambda$ 4026 Å, 4388 Å, 4471 Å, and 4921 Å are expected. This way we want to put at least an upper limit to the He abundance even though no He lines are visible. As can be seen from Table 2 this upper limit tends to be subsolar for the hotter stars, in agreement with the results for blue HB stars in metal-poor clusters (e.g. Moehler et al. 1997, 1999a; Behr et al. 1999).

3.1. Possible errors and discrepancies

1. **Error estimates:** The fit program gives 1σ errors derived from $\Delta\chi^2 = 2.71$ ($T_{\rm eff}$, $\log g$) resp. 3.53 ($T_{\rm eff}$, $\log g$, $\log \frac{n_{\rm He}}{n_{\rm H}}$). However, since χ^2 is not close to 1 these errors will most likely underestimate the true errors. As the errors causing the large χ^2 values are most probably systematic (see below) they are hard to quantify. We decided to get an estimate of their size by assuming that the large χ^2 is solely caused by noise. Increasing σ until $\chi^2 = 1$ then yields new formal errors for $\Delta\chi^2 = 2.71$ and 3.53, respectively, which are given in Table 2. We therefore adopt a general overall error in $\log g$ of ±0.2 dex and in $T_{\rm eff}$ of 5%. Fig. 2 shows theoretical line profiles for the parameters derived for NGC 6441 WF3–17 and model atmosphere spectra for $\Delta\log g = \pm 0.2$ dex.
2. **Large χ^2:** As can be seen from Table 2 the reduced χ^2 is far from 1. We believe that these bad χ^2 values are due to the low resolution of the data (5.7 Å): At $T_{\rm eff}$ = 11,000 K and $\log g = 4$ the FWHM of the theoretical Balmer lines are around 12 Å. Thus the instrumental profile makes up a considerable part of the observed line profile. Therefore any deviations of the instrumental profile from a Gaussian (which is used to convolve the model atmospheres) will lead to a bad fit. Fortunately we could compare the effects for one blue HB star in NGC 6752, for which we have an NTT spectrum with the same setup as is used here and a spectrum from the ESO 1.52m telescope with a resolution of 2.6 Å (for details see Moehler et al. 1999b). Performing a spectroscopic analysis as described above with model atmospheres of [M/H] = −1.5 we find the parameters listed in Table 3. While the χ^2 values for both fits differ considerably the resulting effective temperatures and surface gravities are still rather similar.
3. **Continuum placement:** Using the spectrum of NGC 6441 WF3–17 we checked the effects of a possible misplacement of the continuum: We now normalized the spectrum again, using only the uppermost resp. lowermost continuum points. This amounted to changes of −1% (upper continuum) resp. +3% (lower continuum) in the normalized continuum level. Temperature, gravity and χ^2 were only slightly affected by these changes: In both cases the temperature increased by about 50 K, $\log g$ by 0.03 dex, and χ^2 by about 0.04. The effect of a misplaced continuum is mostly erased by the renormalization of observed *and* model spectrum before fitting, using the same continuum points for both.

The effective temperatures from Table 2 and the $B-V$ colours from Table 1 do not correlate well, esp. for the stars in NGC 6441. However, as the reddening towards these globular clusters is relatively large [$E(B-V) \approx 0.4$ mag] and *may* vary by a few hundredths of a magnitude on small scales (especially in the case of NGC 6441; see Sect. 3.1 in Piotto et al. 1997; for a more general discussion see Heitsch & Richtler 1999), we do not put too much emphasis on this (apparent) inconsistency between spectroscopically derived temperatures and observed (WFPC2) colours.

4. Discussion and Future Work

The atmospheric parameters derived for our programme stars are compared in Fig. 3 to both the canonical ZAHB and the non-canonical tracks for [M/H] = −0.5 from Sweigart & Catelan (1998, 1999, helium-mixed resp. rotation, cf. Sect. 1). Quite unexpectedly, the studied stars

Table 2. Atmospheric parameters and equivalent widths of the Ca II K line for the programme stars for an assumed [M/H] = −0.5. For stars hotter than 9,500 K the first row gives the atmospheric parameters obtained by fitting the Balmer lines and the spectral region of the strongest He I lines. For all stars the first two of the four rows at fixed helium abundance give the solutions on the hot side of the Balmer maximum for the cited helium abundances, while the last two rows give the solutions on the cool side of the Balmer maximum that were rejected because of the strength of the Ca II K line. The errors are 1σ errors adjusted for $\chi^2 > 1$ (see also Sect. 3). A colon marks extrapolated values

Star	χ^2	$T_{\rm eff}$	$\delta T_{\rm eff}$	$\log g$	$\delta \log g$	$\log \frac{n_{\rm He}}{n_{\rm H}}$	$\delta \log \frac{n_{\rm He}}{n_{\rm H}}$	W_λ (Ca II K)	
								obs.	model
		[K]	[K]	[cm s^{-2}]	[cm s^{-2}]			[Å]	[Å]
NGC 6388 WF2–42	4.34	12130	370	4.14	0.12	≤ -2.0	0.6	1.2	0.1
	4.78	12090	310	4.03	0.09	−1.00			
	4.78	12140	320	4.15	0.09	−2.00			
	4.75	7010	70	1.9:	0.26	−1.00			6.5
	4.73	7060	50	2.1:	0.15	−2.00			
NGC 6388 WF3–14	4.12	12250	310	4.56	0.10	≤ -1.9	0.4	3.1	0.1
	3.86	12180	250	4.44	0.07	−1.00			
	3.85	12210	240	4.56	0.07	−2.00			
	3.82	7450	40	2.79	0.08	−1.00			4.2
	3.83	7450	40	2.87	0.07	−2.00			
NGC 6388 WF3–15	2.94	9080	590	3.13	0.34	−1.00		1.7	0.7
	2.94	9130	450	3.26	0.26	−2.00			
	2.94	9100	570	3.14	0.33	−1.00			
	2.94	9160	420	3.29	0.24	−2.00			
NGC 6388 WF4–20	2.18	9960	320	3.71	0.20	≤ -1.5	0.9	1.4	0.3
	1.82	9900	250	3.62	0.12	−1.00			
	1.83	9910	250	3.73	0.12	−2.00			
	1.79	8150	140	2.69	0.07	−1.00			2.5
	1.79	8130	130	2.77	0.06	−2.00			
NGC 6441 WF2–24	2.96	14360	420	5.2:	0.11	≤ -1.8	0.4	3.8	0.1
	3.20	14460	320	5.1:	0.08	−1.00			
	3.28	14400	350	5.2:	0.08	−2.00			
	1.99	7570	20	5.0:	0.11	−1.00			4.1
	2.01	7570	20	5.0:	0.11	−2.00			
NGC 6441 WF3–16	2.61	12710	480	4.65	0.14	≤ -1.8	0.4	3.8	0.1
	2.23	12630	360	4.53	0.10	−1.00			
	2.22	12630	360	4.63	0.10	−2.00			
	1.97	7360	40	3.14	0.15	−1.00			4.2
	1.97	7370	40	3.23	0.15	−2.00			
NGC 6441 WF3–17	2.55	10910	310	4.04	0.15	≤ -1.0	0.5	2.3	0.2
	2.44	10920	250	4.05	0.10	−1.00			
	2.44	10930	250	4.16	0.10	−2.00			
	2.38	7720	70	2.61	0.05	−1.00			3.7
	2.38	7720	70	2.71	0.05	−2.00			

tend to lie preferentially *below* the canonical ZAHB[2]. This behaviour stands in marked contrast to the results for blue HB stars in more metal-poor globular clusters, where lower than canonical gravities are normally found (see Moehler 1999 and references therein). To verify that the high gravities are not due to problems with the low resolution of the data, we also show results for cool blue HB stars in NGC 6752 that were observed during the same run with the same resolution (Moehler et al. 1999b). It can be clearly seen that those stars follow the overall trend seen in NGC 6752 to show lower than expected surface grav-

[2] The difference between Fig. 3 in this paper and Fig. 8 in Moehler (1999) results from using fitting ranges for the preliminary analysis of the line profiles that did not extend far enough to include the wings of the Balmer line profiles.

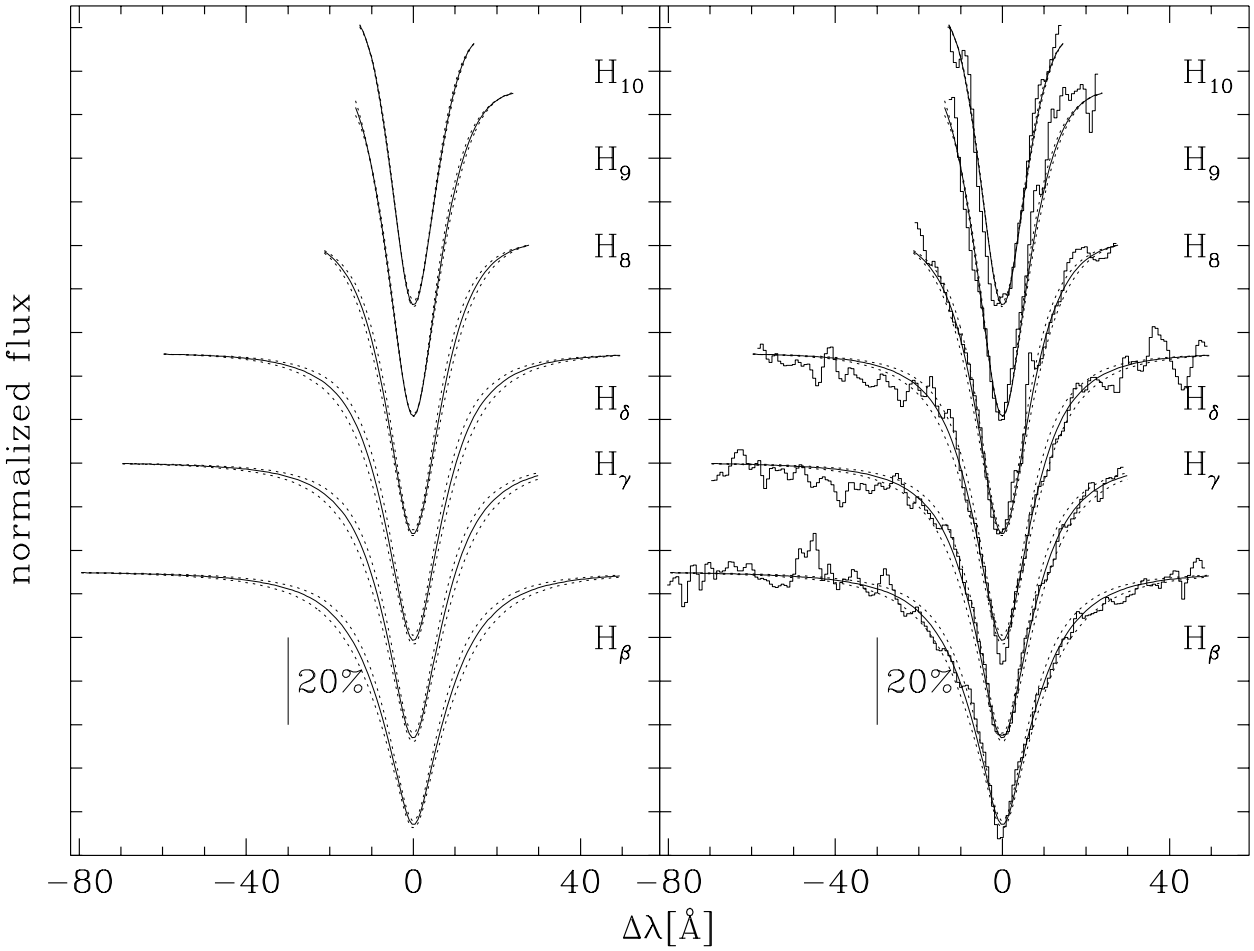

Fig. 2. Plots of model atmosphere spectra for $T_{\rm eff}$ = 10,910 K and log g = 4.04 (solid line), 3.84 (upper dashed line), 4.24 (lower dashed line). The model spectra were convolved by a Gaussian of 5.67 Å FWHM to take into account the instrumental resolution of the observed data. Given are those ranges of the Balmer lines that were fitted to obtain effective temperatures and surface gravities. The asymmetric fit regions are due to the avoidance of He I lines that were fitted separately (see Sect. 3). The right panel shows the observed line profiles of NGC 6441 WF3–17 in comparison

Table 3. Results of spectroscopic analyses for star B 3253 in NGC 6752

	NTT	ESO 1.52m
χ^2	5.09	2.18
$T_{\rm eff}$ [K]	13,630±260	13,810±140
log g [cm s^{-2}]	3.86±0.06	3.99±0.03
log $\frac{n_{\rm He}}{n_{\rm H}}$	−2.2±0.19	−2.7±0.14

ities when fitted with metal-poor model atmospheres. If the high gravities found for the stars in NGC 6388 and NGC 6441 were caused by systematic errors in the data analysis the stars in NGC 6752 should exhibit the same effect.

Considering the estimated errors in $T_{\rm eff}$ and log g the positions of NGC 6388 WF2–42, WF3–14, WF4–20, and NGC 6441 WF3–17, however, are consistent with the canonical ZAHB within 2σ. NGC 6388 WF3–15 could be a blue HB star already on its way to the asymptotic giant branch – as we observed rather bright blue HB stars at the top of the blue tail in both clusters we are biased towards stars evolving from the ZAHB towards higher luminosities. NGC 6441 WF3–16 lies marginally more than 2σ below the unmixed ZAHB, but has also the lowest S/N of all observed stars. NGC 6441 WF2–24 lies 0.7 dex in log g below the canonical ZAHB along the track of a 0.195 $M_\odot$ helium white dwarf (Driebe et al. 1998). In this case it would be a foreground object and most probably member of a binary system having undergone mass transfer, as the low mass single star precursors of helium white dwarfs evolve too slowly to reach this stage within a Hubble time. While helium white dwarfs evolve rather fast and the probability of finding one is therefore rather low, we could not find any other physical explanation for a star like NGC 6441 WF2–24. As we are not able to derive ra-

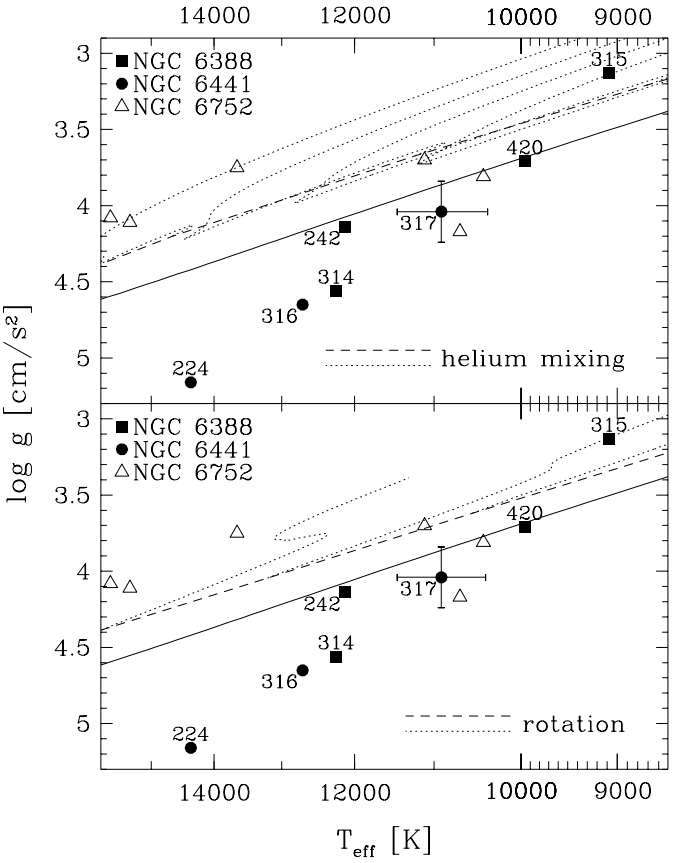

Fig. 3. Comparison of the measured gravities and temperatures for our programme stars in NGC 6388 and NGC 6441 against the HB models for [M/H] = −0.5 from Sweigart & Catelan (1999). The solid curve represents a canonical zero-age HB (ZAHB) for this metallicity. The ZAHB and evolutionary tracks for the sequences which reproduce the observed HB slope in these globular clusters are indicated by the dashed and dotted curves, respectively. The **upper panel** shows the helium-mixed tracks, the **lower panel** shows the rotation tracks. The numbers of the stars refer to Table 2. A representative error bar is plotted at the location of the star NGC 6441 WF3–17. In addition we show cool blue HB stars in NGC 6752, which were observed with the same instrumental setup during the same run (Moehler et al. 1999b)

dial velocities (see Sect. 2) we cannot decide whether this star is a cluster member or not.

The derived gravities (except for NGC 6388 WF3–15) are *significantly* larger than those predicted by the non-canonical tracks that reproduce the upward sloping HB's in the colour-magnitude diagrams of NGC 6388 and NGC 6441 (see Sect. 1). The discrepancy would increase if the atmospheric abundances of the programme stars (and thereby their line profiles) were affected by the radiative levitation of metals (Grundahl et al. 1999). As shown by Moehler et al. (1999a) accounting for this effect moves the parameters of blue HB stars in NGC 6752 to lower temperatures and/or higher gravities. However, the moderate resolution and S/N of the data discussed here do not allow abundances of the heavy elements to be estimated.

We do not have an explanation for this surprising result. All the scenarios laid out by SC98 and discussed in Sect. 1 predict anomalously low gravities for cluster blue HB stars within the temperature range of our programme stars. As far as we are aware, there are no alternative models capable of accounting for the sloped HB's seen in NGC 6388 and NGC 6441 without producing anomalously bright HB stars and hence low gravities. In fact, recent analyses of RR Lyrae variables in NGC 6388 and NGC 6441 (SC98; Layden et al. 1999; Pritzl et al. 1999) *strongly* indicate that the HB's of these globular clusters are substantially brighter than canonical models would predict. Thus we face a conundrum: the non-canonical models which explain the upward sloping HB's in these globular clusters are inconsistent with the derived gravities.

It is clear that further spectroscopic observations of larger (statistically more significant) samples of blue HB stars in NGC 6388 and NGC 6441 are urgently needed to verify the present results.

Acknowledgements. We want to thank the staff of the ESO La Silla observatory for their support during our observations and U. Heber, W.B. Landsman, R. Napiwotzki, and S. Ortolani for their help in improving this paper. Thanks go also to an anonymous referee for valuable remarks. S.M. acknowledges financial support from the DARA under grant 50 OR 96029-ZA. Support for M.C. was provided by NASA through Hubble Fellowship grant HF–01105.01–98A awarded by the Space Telescope Science Institute, which is operated by the Association of Universities for Research in Astronomy, Inc., for NASA under contract NAS 5-26555.

References

Barbuy B., Bica E., Ortolani S., 1998, A&A 333, 117
Behr B.B., Cohen J.G., McCarthy J.K., Djorgovski S.G., 1999, ApJ 517, L135
Bergeron P., Saffer R.A., Liebert J., 1992, ApJ 394, 228
Bressan A., Chiosi C., Fagotto F., 1994, ApJS 94, 63
Caloi V., 1989, A&A 221, 27
Catelan M., de Freitas Pacheco J.A., 1996, PASP 108, 166
Dorman B., O'Connell R.W., Rood R.T., 1995, ApJ 442, 105
Driebe T., Schönberner D., Blöcker T., Herwig F., 1998, A&A 339, 123
Greggio L., Renzini A., 1990, ApJ 364, 35
Greggio L., Renzini A., 1999, MmSAI 70, 691
Grundahl F., Catelan M., Landsman W.B., Stetson P.B., Andersen M.I., 1999, ApJ, in press (October 1999) (`astro-ph/9903120`)
Hamuy M., Walker A.R., Suntzeff N.B., Gigoux P., Heathcote S.R., Phillips M.M., 1992, PASP 104, 533
Harris W.E., 1996, AJ 112, 1487 (`http://physun.physics.mcmaster.ca/Globular.html`, version of June 22, 1999)

Heitsch F., Richtler T., 1999, A&A 347, 455
Horne K., 1986, PASP 98, 609
Kraft R.P., 1994, PASP 106, 553
Kurucz R.L., 1991, private communication
Layden A.C., Ritter L.A., Welch D.L., Webb T.M.A., 1999, AJ 117, 1313
Minniti D., 1995, AJ 109, 1663
Minniti D., 1996, ApJ 459, 175
Moehler S., 1999, RvMA 12, p. 281
Moehler S., Heber U., Rupprecht G., 1997, A&A 319, 109
Moehler S., Sweigart A.V., Landsman W.B., Heber U., Catelan M., 1999a, A&A 346, L1
Moehler S., Sweigart A.V., Landsman W.B., Heber U., 1999b, in prep.
Ortolani S., Renzini A., Gilmozzi R., Marconi G., Barbuy B., Bica E., Rich R.M., 1995, Nat 377, 701
Piotto G., et al., 1997, HST Observations of High-Density Globular Clusters. In: Rood R.T., Renzini A. (eds.), Advances in Stellar Evolution. Cambridge University Press, Cambridge, p. 84
Pritzl B., Smith H.A., Catelan M., Sweigart A.V., 1999, in preparation
Rich R.M., 1998, The Galactic Bulge. In: Sofue Y. (ed.), Proc. IAU Symp. 184, The Central Region of the Galaxy and Galaxies. Kluwer, Dordrecht, p. 11
Rich R.M., et al., 1997, ApJ 484, L25
Rood R.T., Crocker D.A., 1989, Horizontal Branch Evolution. In: Schmidt E.G. (ed.), The Use of Pulsating Stars in Fundamental Problems of Astronomy. Cambridge University Press, Cambridge, p. 103
Saffer R.A., Bergeron P., Koester D., Liebert J., 1994, ApJ 432, 351
Sweigart A.V., 1997, Helium Mixing in Globular Cluster Stars. In: Philip A.G.D., Liebert J., Saffer R.A. (eds.), The Third Conference on Faint Blue Stars. L. Davis Press, Schenectady, p. 3
Sweigart A.V., Catelan M., 1998, ApJ 501, L63 (SC98)
Sweigart A.V., Catelan M., 1999, in prep.
Tüg H., 1977, ESOMe 11, 7
Yi S., Demarque P., Oemler A., 1998, ApJ 492, 480
Zinn R., 1996, The Galaxy's Globular Clusters. In: Morrison H., Sarajedini A. (eds.), ASP Conf. Ser. 92, Formation of the Galactic Halo....Inside and Out. Astronomical Society of the Pacific, San Francisco, p. 211